Supporting information

(20 pages, 12 figures, 1 table)

Zinc in House Dust:

Speciation, Bioaccessibility and Impact of Humidity

Suzanne Beauchemin[1], Pat E. Rasmussen[2,3], Ted MacKinnon[1], Marc Chénier[2] and Kristina Boros[3]*

1. Natural Resources Canada, CanmetMINING, 555 Booth Street, Ottawa, Ontario, Canada, K1A 0G1
2. Environmental Health Science and Research Bureau, HECSB, Health Canada, 50 Columbine Driveway, Tunney's Pasture 0803C, Ottawa, Ontario, Canada, K1A 0K9
3. University of Ottawa, Earth Sciences Department, Ottawa, ON

*corresponding author: sbeauche@nrcan.gc.ca

APPENDIX A: MATERIALS and METHODS

Zn reference compounds

A comprehensive suite of 29 Zn reference compounds were purchased, acquired from mineral collections or synthesized for XAS characterization and modeling of the samples. These compounds represent Zn species occurring as primary minerals (e.g., Zn silicates, franklinite) and secondary species (e.g., sorbed species, Zn-rich phyllosilicates) in soils impacted by industrial activities, as well as Zn compounds used in manufacturing processes and commercial products (e.g., metal Zn, ZnO, ZnS). Table A1 provides an overview of the standards, while Figures A1 to A5 illustrate their XANES and EXAFS spectra. Two-line ferrihydrite and birnessite were synthesized according respectively to the procedures described in Schwertmann and Cornell (1991) and Beak et al. (2008). The precipitates were left to age for 48 hours under N_2 atmosphere at room temperature, then washed, centrifuged, and resuspended in 10 mM KCl at pH 6.5 for adsorption experiments. Gibbsite (Wards Research Mineral) and kaolinite (Source clays repository from the Clay Mineral Society, low defect KGa-1b, BET=10 m^2/g) were suspended in 10 mM KCl at pH 6.5. All four minerals were analyzed by XRD for purity check. Zn was adsorbed at an initial rate of 800 mmol/kg on ferrihydrite and birnessite, while lower rates of 300 mmol/kg for gibbsite and 100 mmol/kg for kaolinite were used. Final concentrations of Zn adsorbed species were: 582 mmol/kg ferrihydrite, 673 mmol/kg birnessite, 1.8 mmol/kg gibbsite and 6 mmol/kg kaolinite. The procedure for Zn adsorbed on humate was adapted from the one described for Pb in Beauchemin et al. (2011). Zn was adsorbed on cystein at a molar ratio S/Zn = 10 at pH 7.0 (Beauchemin et al. 2004). Zn was adsorbed on lignin (purchased) at the initial concentration of 15 mmol/kg at pH 7.5. Zn-Al layered double hydroxide (Zn_LDH) was synthesized by titrating a solution of 30 mM $ZnCl_2$ with 1 mM $AlCl_3$ at pH 6.5, according to the procedure of Taylor (1984) and using a molar Zn:Al ratio of 3:1 as in Ford and Sparks (2000). The Zn-rich phyllosilicate was synthesized according to the protocol of Hayes et al. (2011).

Bulk XAS analysis

The XAS analyses were conducted at the beamline X-11A at the National Synchrotron Light Source, Brookhaven National Laboratory, New York. All reference materials were diluted in boron nitride (BN), except for Zn naphthenate diluted in Vaseline, to a concentration yielding an edge step of 1 in transmission mode and mounted behind Kapton tape in acrylic plexiglass holders. Data for standards were collected in transmission mode using ion chambers. The dust samples were analyzed without

dilution in fluorescence mode using a solid-state, multi-element germanium detector. Between five and seven scans were collected and averaged for each sample. The Si(111) monochromator was calibrated at the Zn K-edge using the first peak of the first derivative XANES spectrum for the Zn foil (9659 eV). The energy scale for each sample was also referenced to the edge in the spectrum for Zn foil collected in transmission mode simultaneously with sample data. The XANES data were processed, baseline corrected and normalized using Athena 8.061 (Ravel and Newville, 2005).

Weathering experiment I: Principal component analysis (PCA) and target transformation analysis were initially carried out on the dataset composed of all 6 EXAFS spectra of the dust samples from the first experiment (C_043, H_112, N_2584; before and after weathering; range of 2 to 10.5 Å^{-1}), using the same approach as described in Beauchemin et al. (2002). PCA provides a statistical basis for choosing the number of standard species to include in the least-squares, linear combination fitting (LCF), while target transformation provides statistical basis to reject or accept a given Zn reference compound and help reduce LCF to a smaller subset of standards. For the first weathering experiment, the IND function and F test in the PCA showed that the first three components (n=3) were significant and explained 98.4% of the variance in the experimental dataset. Using these 3 components, target transformation analysis was conducted to test individually each of the 28 reference compounds (EXAFS spectrum for SphalAP was similar to that of ZnS_pow, and therefore only ZnS_pow was included in the analysis– Fig. A4). Zn species with SPOIL values > 6 were discarded as unacceptable species (Zn metal, ZnFeO_100, franklin). Likewise, species with marginal SPOIL values between 3 and 6 also showing a probability of F < 0.01 (ZnCO₃, ZnF₂, hemimorphy, Zn_phyllo) were rejected, leaving a subset of 21 standards for LCF. After initial LCF analyses with the 21 standards, 6 reference species were later discarded as they did not come out as potential species in the solution (Znnapht, ZnBiCo, Willem, Zn_LDH, Zn_kaolin, Zncarbam). Therefore, LCF was finally performed on the Zn EXAFS chi data (k=3) of the dust sample using all possible binary and ternary combinations of the remaining 15 retained Zn reference standards. LCF was done using Athena 8.061. The EXAFS fitting ranged from 2 to 10.5 A^{-1}. No energy shift was allowed for the EXAFS fitting and no constraint to sum to 1 was imposed. R-factor and reduced chi-squared values were adopted as goodness-of-fit criteria. The best combinations obtained on the EXAFS chi data were then tested for reliability by fitting the normalized XANES spectra over the relative energy range of -30 to 100 eV. No energy offset parameters were included in the fitting of XANES and no constraint to sum to 1 were imposed.

Weathering experiment II

The same approach as described above was adopted for modeling the bulk XAS analyses of the weathered Faraday samples spiked with various Zn species. In brief, PCA was initially carried out on the dataset composed of all 7 EXAFS spectra of the Faraday dust samples (original Faraday dust before and after weathering, Faraday spiked with ZnS_pow, ZnO_pow, ZnO_10, Zn_Fh or $ZnSO_4$ after weathering for 5 months; chi range of 2.5 to 10 Å^{-1}). Based on IND function and F test, the first two components (n=2) were significant and explained 97.4% of the variance in the experimental dataset. Target transformation analysis was performed using these first 2 components to test each of the 28 Zn reference compounds. Target transformation analysis indicated that only ZnS_pow and Zn_cysteine were acceptable targets (SPOIL values < 3); Znnaphth, Zncarbam, ZnPO4, Zn_lignin, Zn_Fh and Zn_stear had marginal SPOIL values between 3 and 6, with F probabilities < 0.001. All other species were unacceptable, including spiked species of ZnO_pow and ZnO_10 (SPOIL value > 6; F probabilities < 0.0001). These results reflected a lack a sensitivity of this approach for this fairly homogeneous dataset of all Faraday samples, as observed in some similar cases (Manceau et al., 2002; Beauchemin et al., 2003). For this reason, Zn species with SPOIL values up to 6 were retained for LCF, except for Znnapht and Zncarbam which were shown as unlikely targets in dust samples from the first experiment. In addition, several Zn standards considered unacceptable (SPOIL values > 6) were nevertheless integrated in the LCF to include species used in spiking the Faraday dust (e.g. ZnO_pow, ZnO_10, $ZnSO_4$), as well as species commonly found in dust (Zn hyd. carb), and organic and sorbed species that might occur as secondary reactions with the dust matrix (Znoxalat, Znacetat, Znstearat, Zn_humate, Zn_gibb, Zn_birn). In the end, LCF was performed on the Zn EXAFS chi data (k=3) of the dust sample using all possible binary and ternary combinations of the same 15 Zn reference standards as retained for experiment I. The EXAFS and XANES fitting was done as described above for experiment I.

Table A1. Overview of the 29 Zn reference compounds characterized for XAS modeling.

	Label	Description / expected formula	Origin	XRD purity check
A. **Purchased inorganic compounds**				
1	Zn_metal	elemental Zinc, powder	Alfa Aesar #00424	elemental Zn
2	ZnO	ZnO - zincite, mesh powder	Alfa Aesar #11137	ZnO - zincite
3	ZnO_10	ZnO 8-10 nm particle size	Alfa Aesar #44299	ZnO - zincite
4	ZnS	ZnS - sphalerite; mesh powder	Alfa Aesar #40091	ZnS - sphalerite
5	ZnFeO_100	Zn iron oxide < 100 nm particle size	Sigma-Aldrich #633844	$ZnFe_2O_4$ - franklinite
6	Zn hyd. carb.	Zinc hydroxide carbonate	Alfa Aesar; #33398	$Zn_5(OH)_6(CO_3)_2$ - Hydrozincite
7	ZnCO3	$ZnCO_3$ - smithsonite	Ward Research Mineral	$ZnCO_3$ - smithsonite
8	ZnPO4	$Zn_3(PO_4)_2$ - Zn phosphate	Alfa Aesar #13013	$Zn_3(PO_4)_2$ - Zn phosphate dominant + Zn ortho phosphate $Zn_3(PO_4)_2(H_2O)_4$ and $Zn_3(PO_4)_2(H_2O)$
9	ZnSO4	$ZnSO_4.7H_2O$	Alfa Aesar #33399	Bianchite $ZnSO_4.6H_2O$
10	ZnF2	ZnF_2 (anhy)	Alfa Aesar #12986	ZnF_2 - Zinc fluoride
11	ZnBiCo_nano	Bismuth cobalt zinc oxide <100 nm particle size; $(Bi_2O_3)0.07(CoO)0.03(ZnO)0.90$	Sigma Aldrich #631930	$Bi_2O_3 + Bi_{24}CoO_{37} + ZnO + Bi_2(CO_3)O_2 + Co(II)O$
B. **Purchased organic compounds**				
12	Znoxalat	Zn oxalate	Alfa Aesar #12985	n.a: Not available
13	Znacetat	Zn acetate dihydrate	Alfa Aesar #11559	n.a.
14	Znstearat	Zn stearate (Zn octadecanoate)	Alfa Aesar #33238	n.a.
15	Znnaphth	Zn naphthenate	Alfa Aesar #39554	n.a.
16	Zncarbam	Zn diethyldithiocarbamate C10-H20-N2-S4.Zn; 17-19.5% Zn	Alfa Aesar #18697	n.a.

Table A1 continued. Overview of the 29 Zn reference compounds characterized for XAS modeling.

C. **Synthesized at Canmet*MINING***				
17	Zn_Fh	Zn adsorbed on 2-line ferrihydrite; pH 6.5; 800 mmol Zn/kg; final: 582 mmol/kg	Synthesized SB lab Oct 2011 to May 2012	2-line ferrihydrite - $Fe(OH)_3$
18	Zn_birn	Zn adsorbed on birnessite; pH 6.5; 800 mmol Zn/kg; final: 673 mmol/kg	Synthesized SB lab Oct 2011 to May 2012	Birnessite - MnO_2
19	Zn_gibb	Zn adsorbed on gibbsite; pH 6.5; 300 mmol Zn /kg; final 1.8 mmol/kg	Synthesized SB lab Oct 2011 to May 2012	Gibbsite - $Al(OH)_3$
20	Zn_humate	Zn adsorbed on humate; pH 6; 300 mmol Zn/kg; final = 112 mmol/kg	Synthesized SB lab Oct 2011 to May 2012	n.a.
21	Zn_LDH	Zn Al double layered hydroxide; pH 6.5; final concentration 6754 mmol Zn /kg	Synthesized SB lab Oct 2011 to May 2012	XRD pattern shows crystalline peaks -
22	Zn_phyllo	Zn-rich phyllosilicate (Zn talc); final concentration 5898 mmol Zn/kg	Synthesized SB lab Oct 2011 to May 2012	XRD pattern shows amorphous + crystalline peaks -
23	Zn_kaolin	Zn adsorbed on kaolinite; pH 6.5; 100 mmol Zn /kg; final: 6 mmol/kg	Synthesized SB lab Oct 2011 to May 2012	Well characterized Kaolin, Clay Mineral Society (CO, USA)
24	Zn_lignin	Zn adsorbed on lignin; pH 7.5; 15 mmol Zn/kg	Synthesized SB lab June 2002 - unpublished	n.a.
25	Zn_cysteine	Zn adsorbed on cystein; molar ratio S/Zn = 10; pH 7.0	Synthesized SB lab March 2003; Beauchemin et al. 2004	n.a.

Table A1 continued. Overview of the 29 Zn reference compounds characterized for XAS modeling.

D. **Natural minerals**				
26	Hemimorph	Hemimorphite $Zn_4Si_2O_7(OH)2.H_2O$	CANMET library; CANMET: Friedensville Zinc Mine, Friedensville, PA	Hemimorphite; pretty pure: theoretical concentration in Zn = 54.3 wt.% vs. measured = 54.6 wt.%
27	Willemit	Willemite - Zn_2SiO_4	CANMET library ; CANMET: Franklin, NJ; Willemite, calcite, rhodonite, franklinite	Willemite + minerals not bearing Zn: calcite, fluorite (CaF_2); substantial dilution by matrix: theoretical concentration in Zn = 58.7 wt.% vs. measured = 10 wt.%
28	Franklin	Franklinite - $ZnFe_2O_4$	Alfa Aesar #19407	Franklinite + slight oxidation as ZnO
29	SphalAP	Sphalerite - ZnS (7% Fe)	Natural mineral from Dr. A. Pratt (Canmet*MINING*) with 60% Zn and 7% Fe	Sphalerite
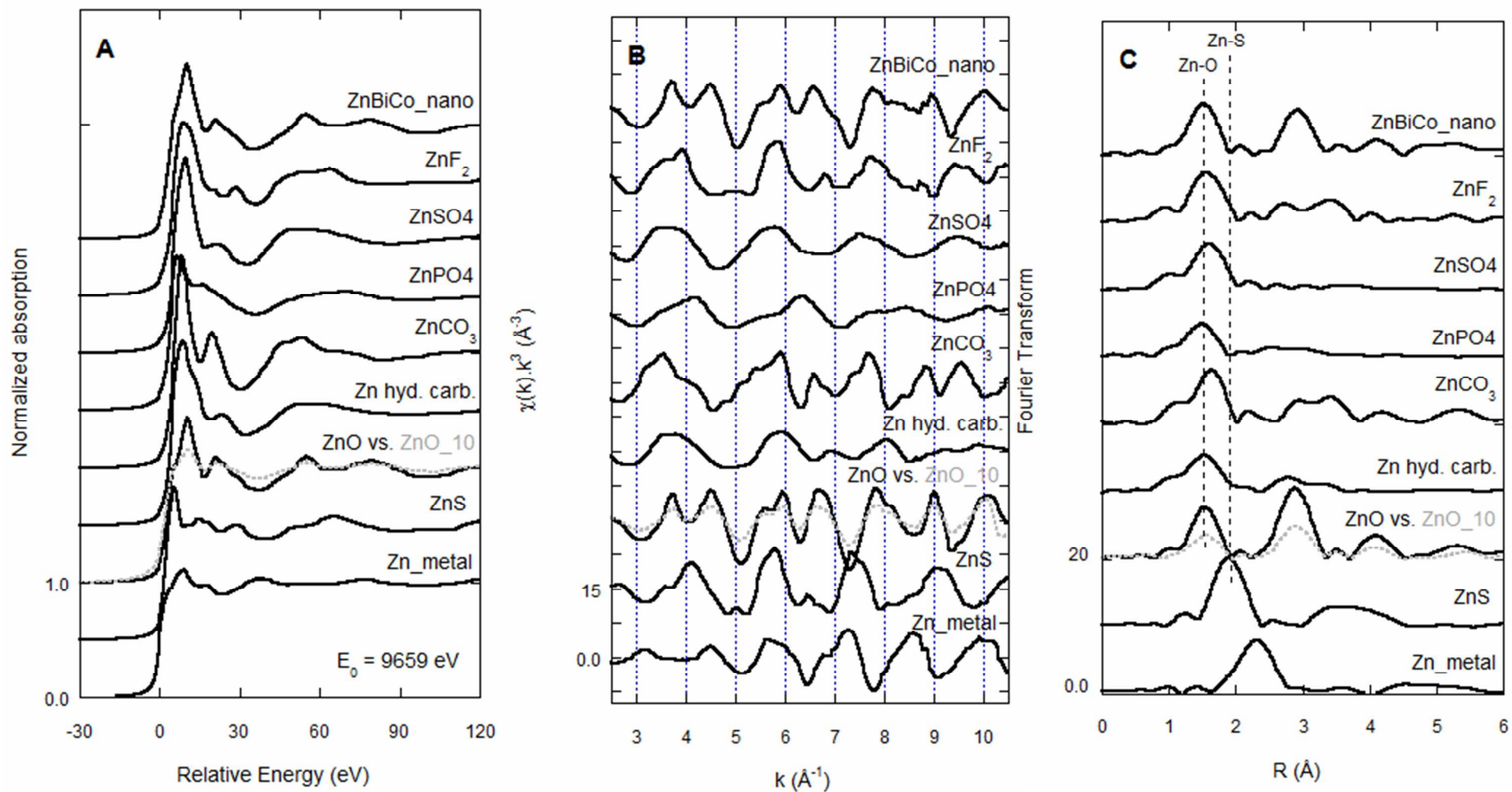
Figure A1. (A) Zn K-edge XANES, (B) k^3-weighted EXAFS and (C) Fourier transformed k^3-weighted EXAFS (uncorrected for phase shift) for the purchased inorganic Zn reference compounds (labels as in Table A1). For ZnO: solid black line = mesh powder; dotted grey line = ZnO_10 nm. Compared to ZnO mesh powder, ZnO nanoparticles show lower peak intensity in the XANES, chi and FT spectra.
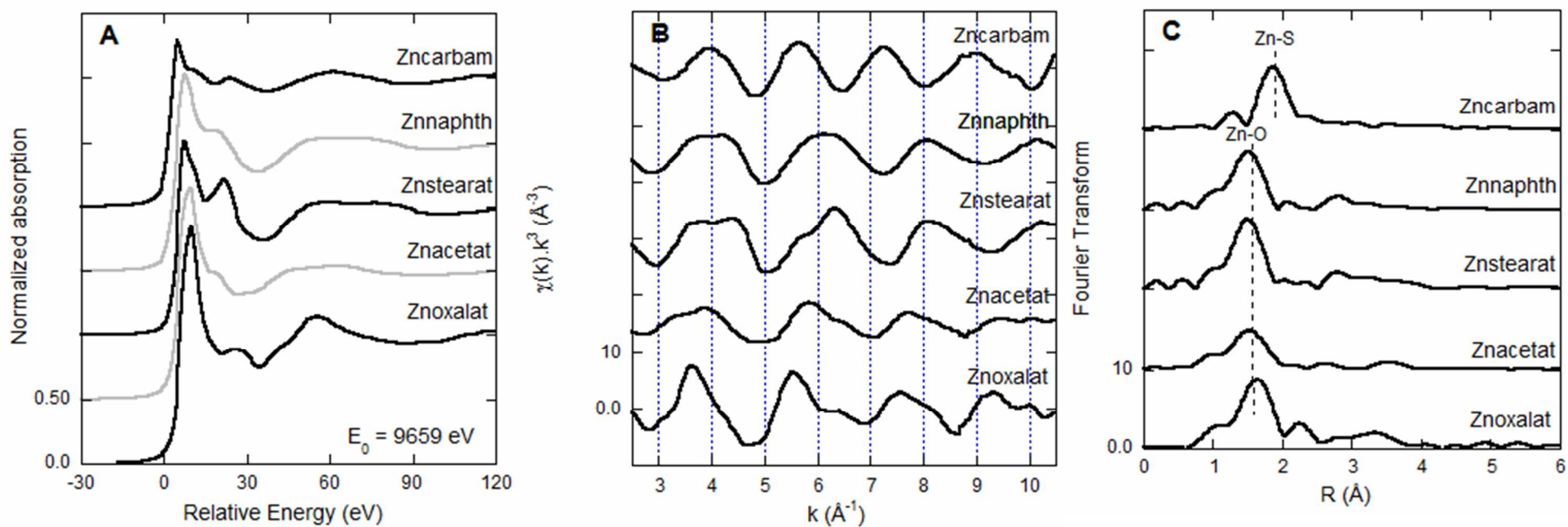
Figure A2. (A) Zn K-edge XANES, (B) k^3-weighted EXAFS and (C) Fourier transformed k^3-weighted EXAFS (uncorrected for phase shift) for the purchased organic Zn reference compounds (labels as in Table A1).
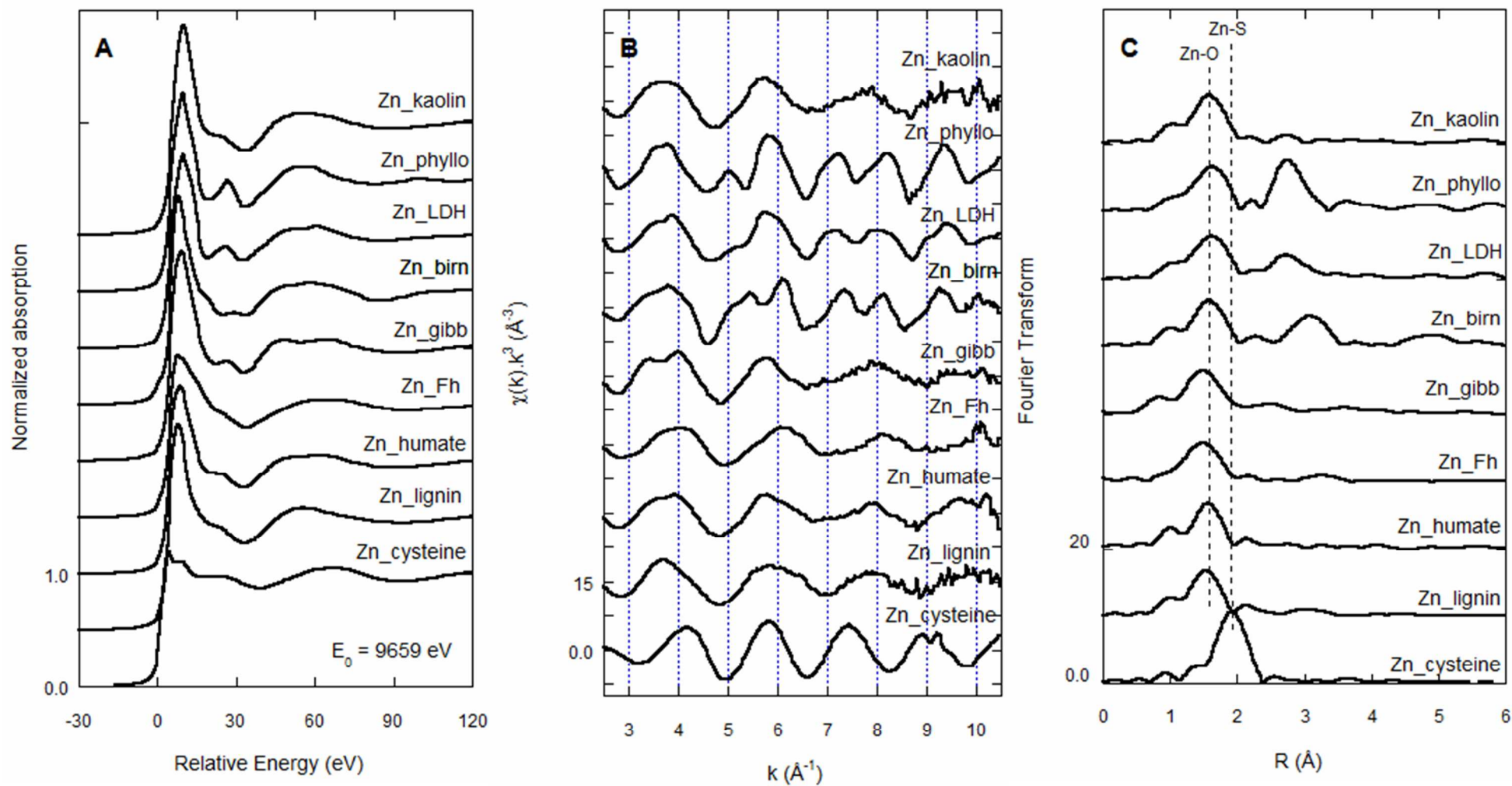
Figure A3. (A) Zn K-edge XANES, (B) k^3-weighted EXAFS and (C) Fourier transformed k^3-weighted EXAFS (uncorrected for phase shift) for the Zn reference compounds synthesized at CanmetMINING (labels as in Table A1).
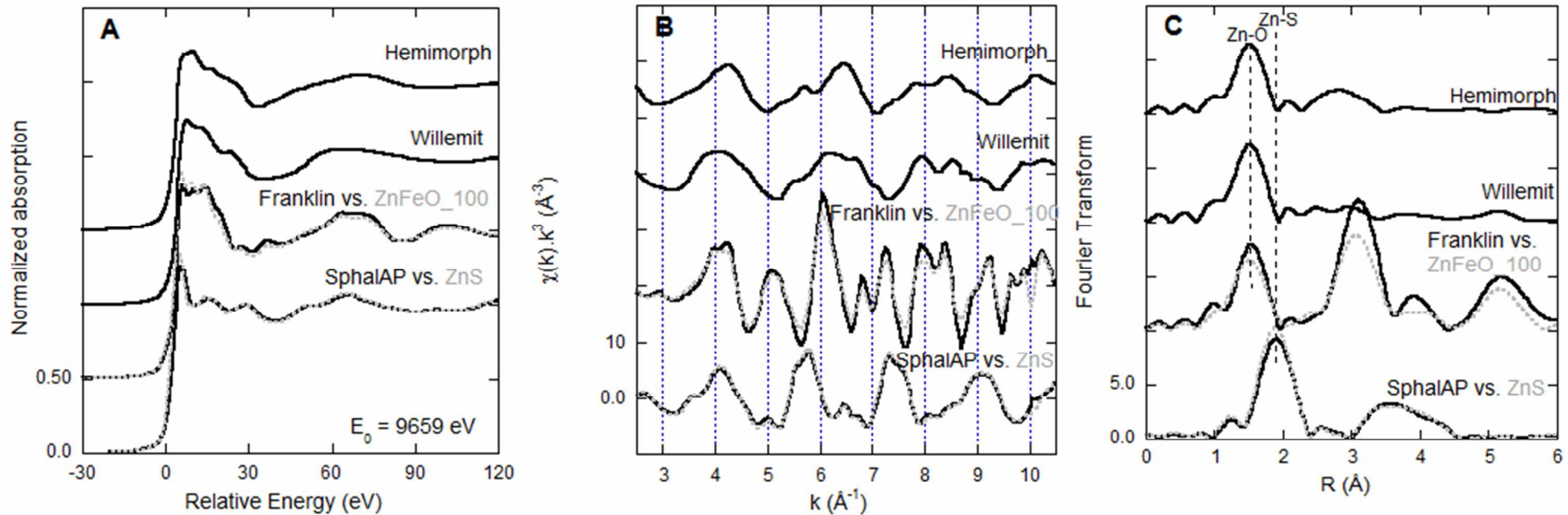
Figure A4. (A) Zn K-edge XANES, (B) k^3-weighted EXAFS and (C) Fourier transformed k^3-weighted EXAFS (uncorrected for phase shift) for the natural Zn-bearing minerals (labels as in Table A1). Franklinite (Franklin; solid black line) is compared with the purchased Zn iron oxide nanoparticles (ZnFeO_100; dotted grey line); the nanoparticles tend to have lower amplitude in the chi and FT spectra compared to the natural mineral. The sphalerite mineral (SphalAP; solid black line) exhibit the same XANES, chi and FT spectra than the purchased ZnS powder (ZnS; dotted grey line).
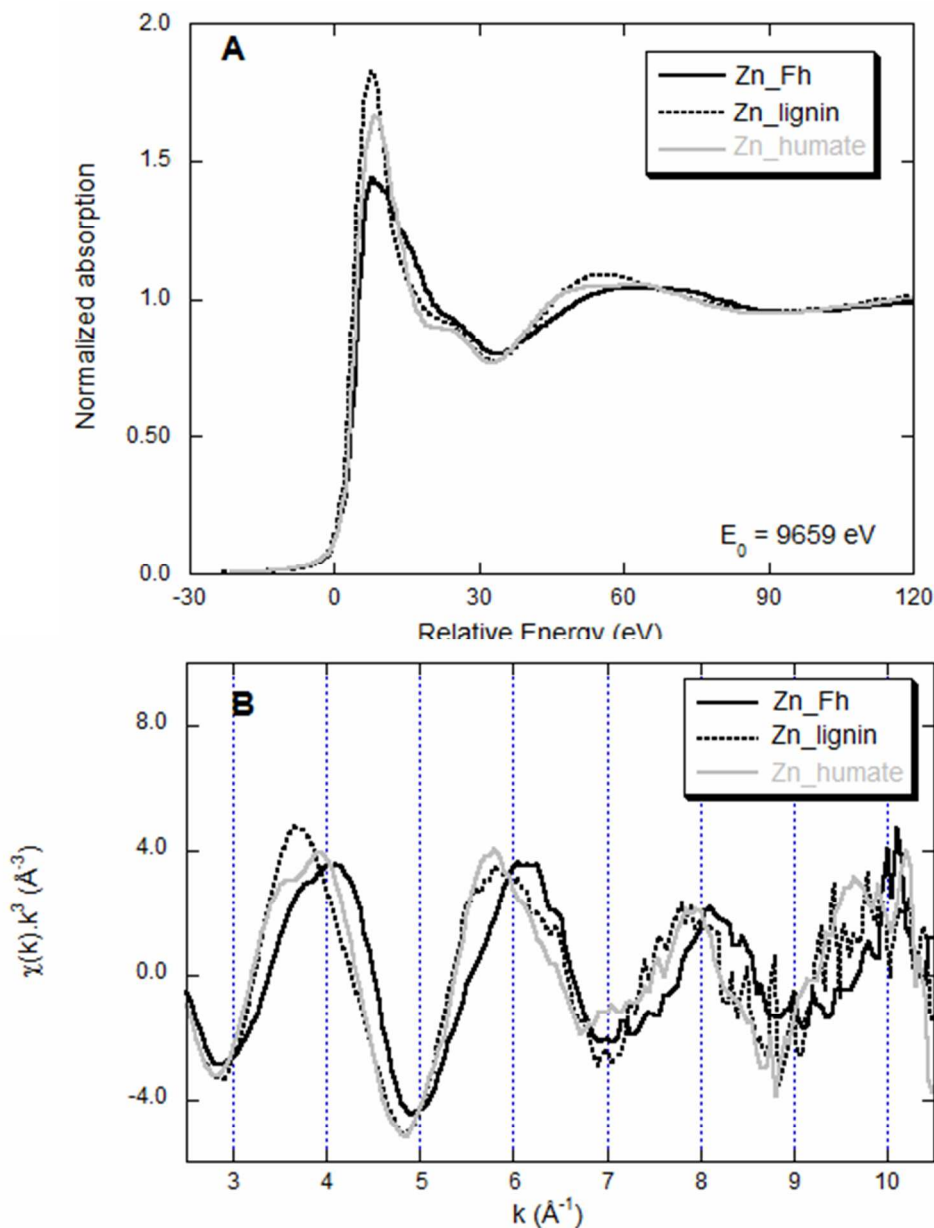
Figure A5. Comparison of the (A) Zn K-edge XANES and (B) k^3-weighted EXAFS spectra for Zn adsorbed on ferrihydrite (Zn_Fh), on humate and on lignine. XANES and EXAFS spectra for Zn_Fh differ from those of Zn species adsorbed on organic matter: the chi data for Zn_Fh are shifted to the right while XANES shows a shoulder on the high energy side of the white line. Differences can be observed between Zn_humate and Zn_lignin but they are more subtle: Zn_humate has more pronounced XANES features and a more structured first oscillation at 3.5 Å^{-1} in its chi spectrum, compared to Zn_lignin. Given the subtility of these differences, the generic term "Zn adsorbed on organic matter" is usually used in the discussion. Microspectroscopic analysis with µXRF and µXANES provides additional support to distinguish between Zn sorbed to Fe-oxides and organic matter, based on the Fe signal in the µXRF (e.g., Fig. A6, spot 4; Fig. A7, spot 2).
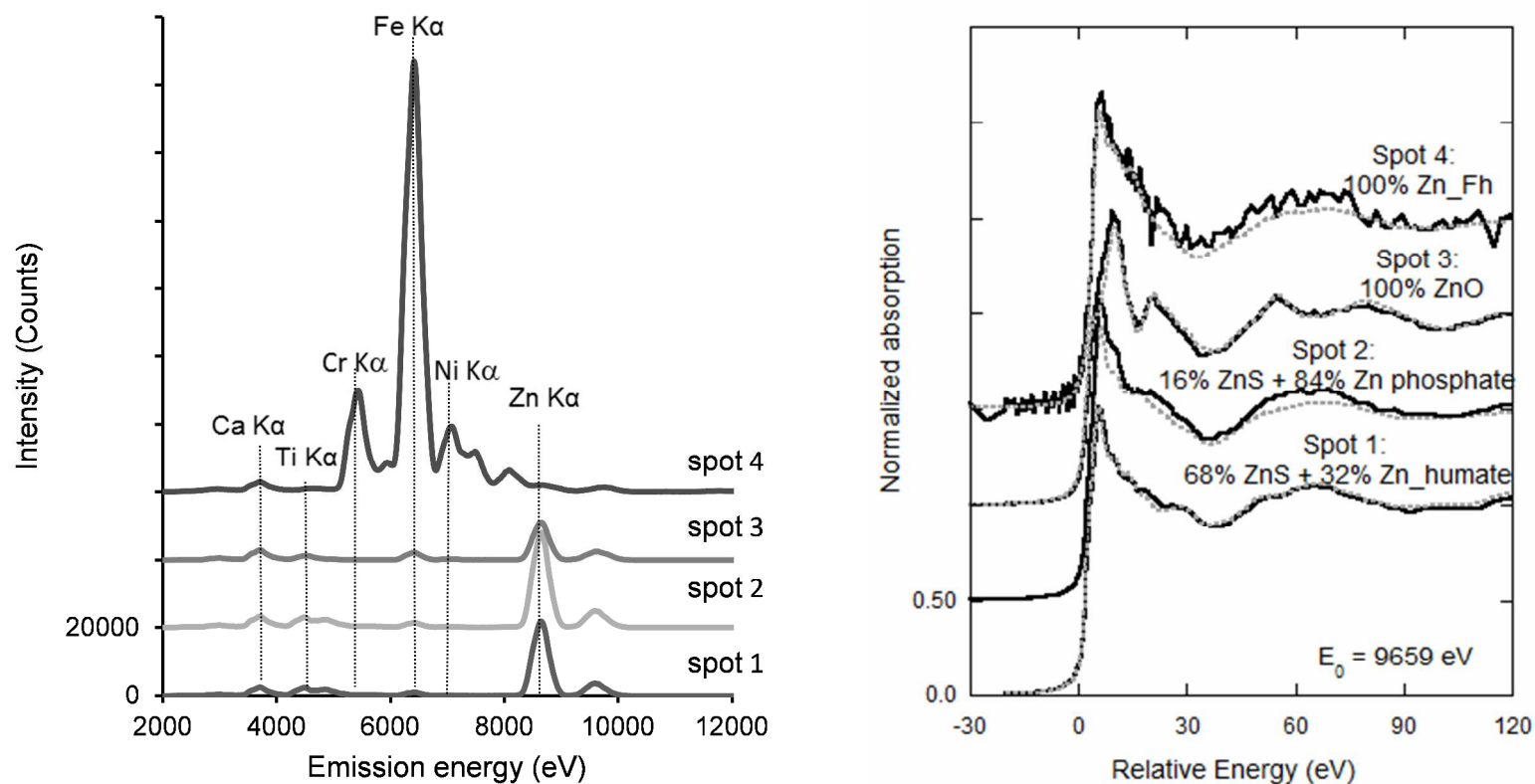
Figure A6. µXRF spectra at E = 9.8 KeV (left) and µXANES spectra at the Zn K-edge (right) of four spots from a map of the original sample H_112; solid lines = measured data; dotted grey lines = fitted data. (Zn_Fh= Zn adsorbed on ferrihydrite; Zn_humate= Zn adsorbed on humate).
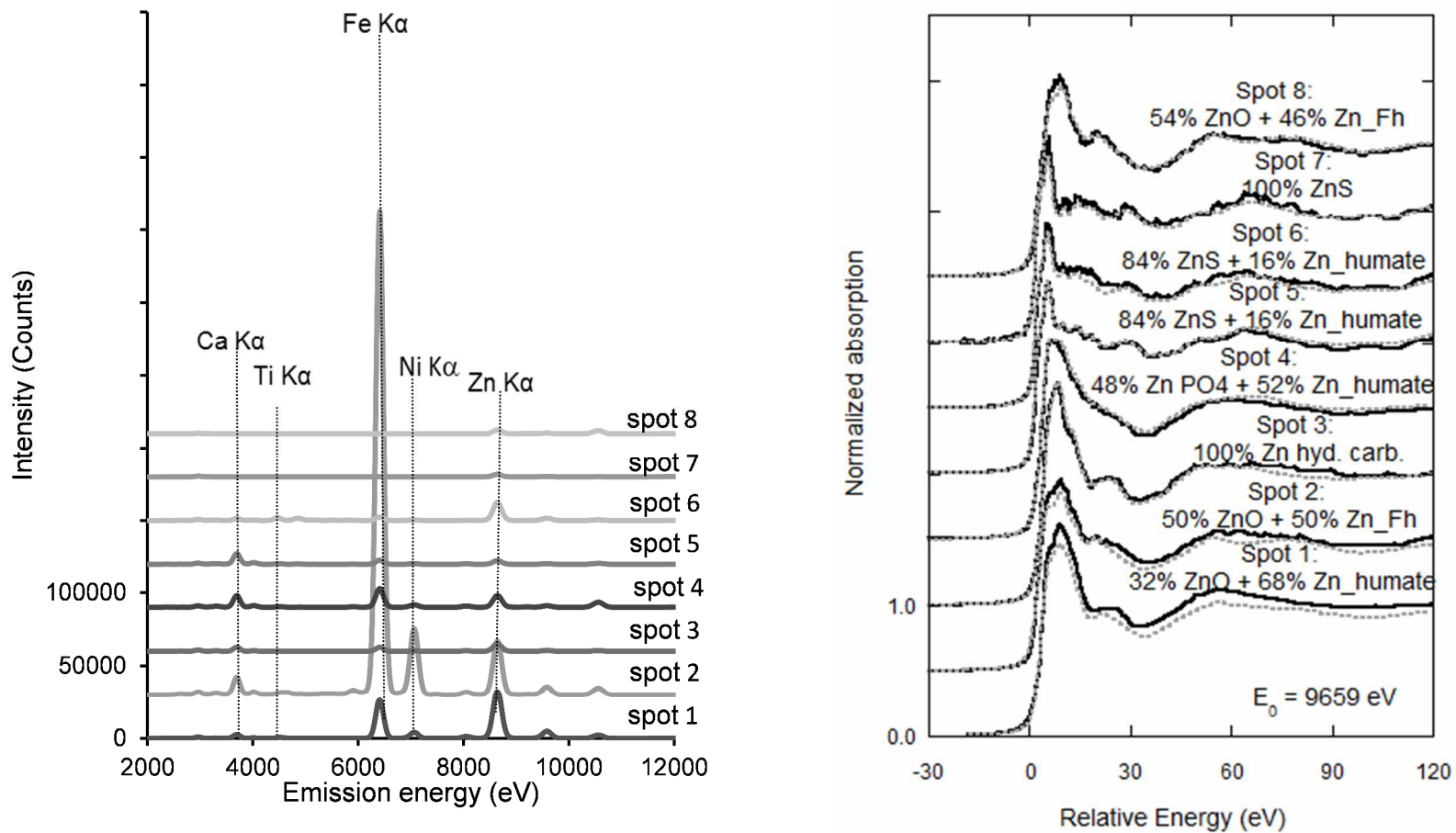
Figure A7. µXRF spectra at E = 13.5 KeV (left) and µXANES spectra at the Zn K-edge (right) of six spots from a map of the 4-month weathered sample H_112; solid lines = measured data; dotted grey lines = fitted data. (Zn_Fh= Zn adsorbed on ferrihydrite; Zn_humate= Zn adsorbed on humate; Zn hyd. carb.= Zn hydroxyl carbonate; Zn PO4 = Zn phosphate).
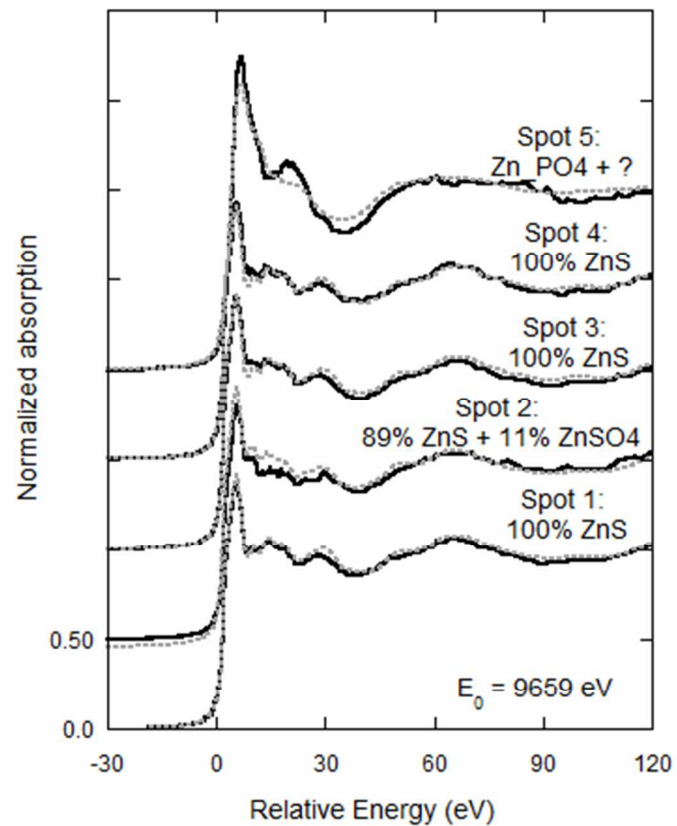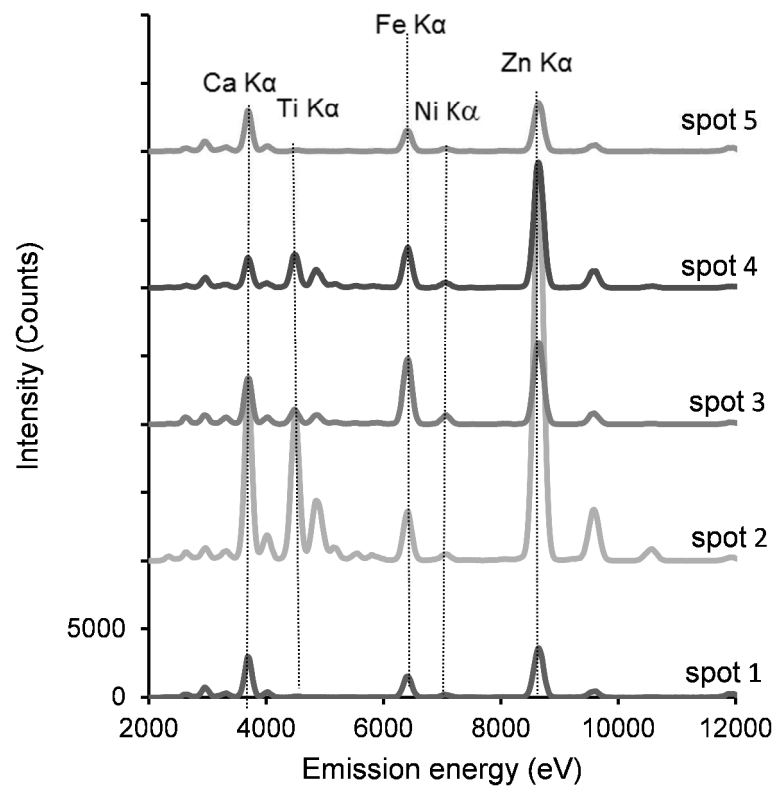
Figure A8. μXRF spectra at E = 13.5 KeV (left) and μXANES spectra at the Zn K-edge (right) of five spots from a map of the original Far dust sample; solid lines = measured data; dotted grey lines = fitted data. (Zn_PO4 = Zn phosphate).
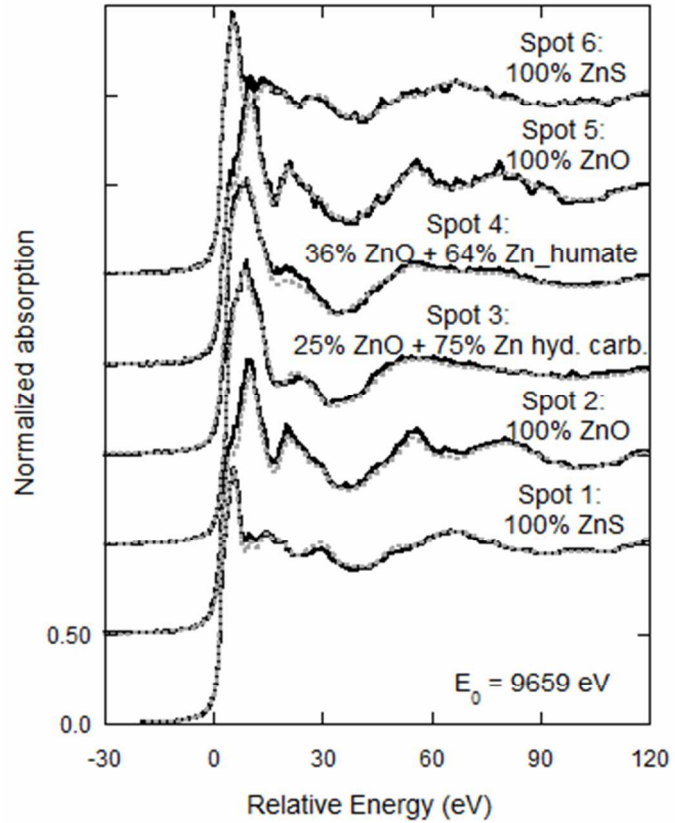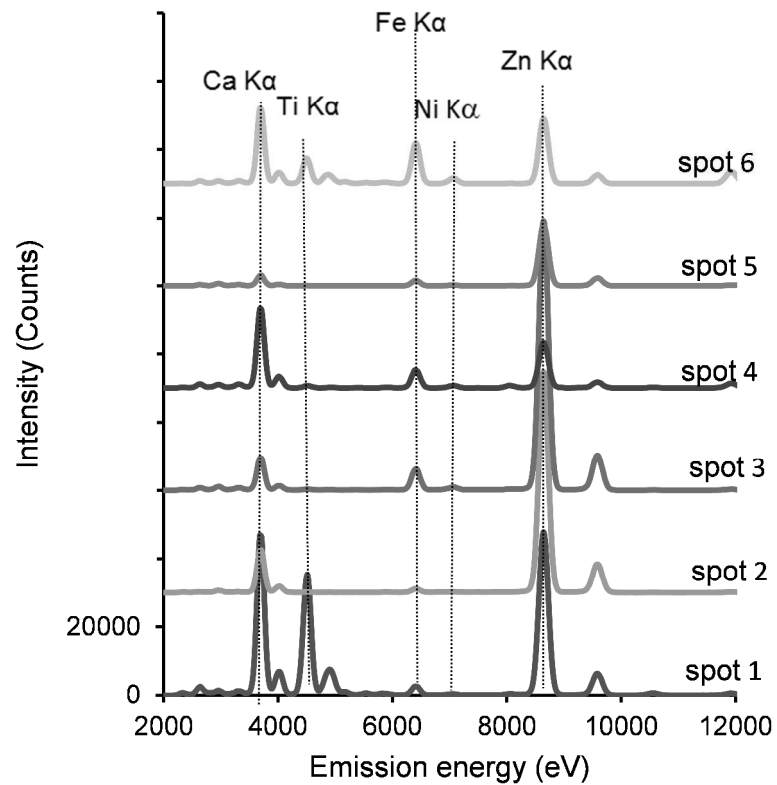
Figure A9. µXRF spectra at E = 13.5 KeV (left) and µXANES spectra at the Zn K-edge (right) of six spots from a map of the 5-month weathered Far dust sample; solid lines = measured data; dotted grey lines = fitted data. (Zn_humate= Zn adsorbed on humate; Zn hyd. carb.= Zn hydroxyl carbonate).
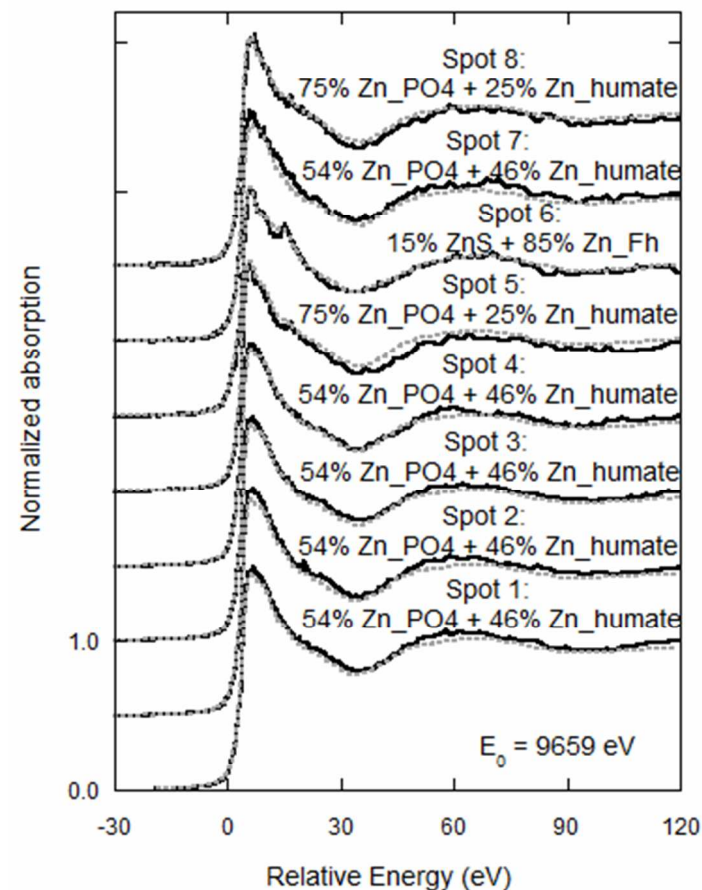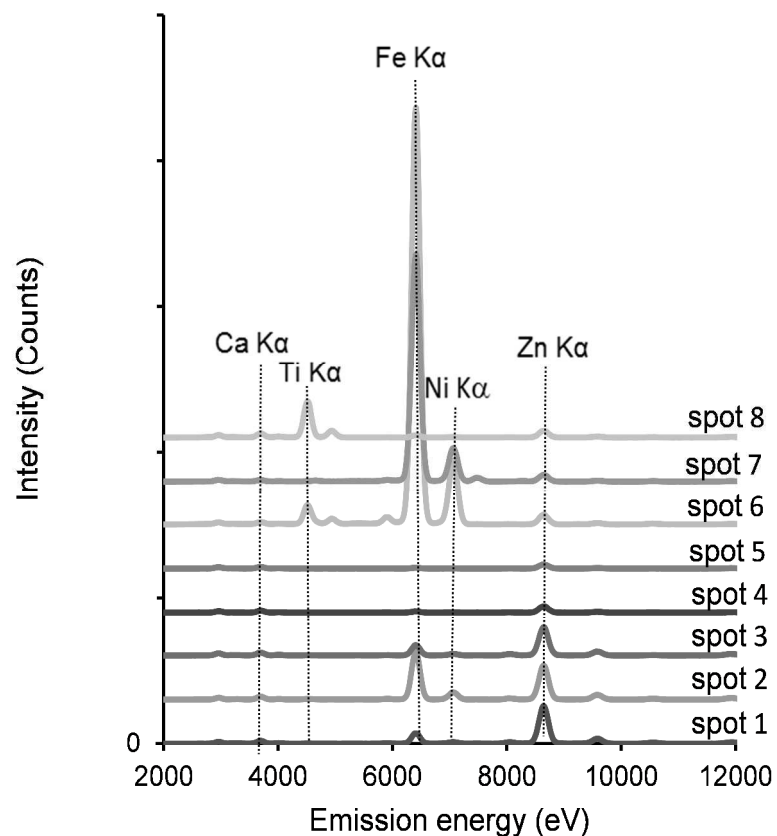
Figure A10. µXRF spectra at E = 13.5 KeV (left) and µXANES spectra at the Zn K-edge (right) of eight spots from a map of the weathered Far dust sample spiked with ZnO; solid lines = measured data; dotted grey lines = fitted data. (Zn_Fh= Zn adsorbed on ferrihydrite; Zn_humate= Zn adsorbed on humate; Zn_PO4 = Zn phosphate).
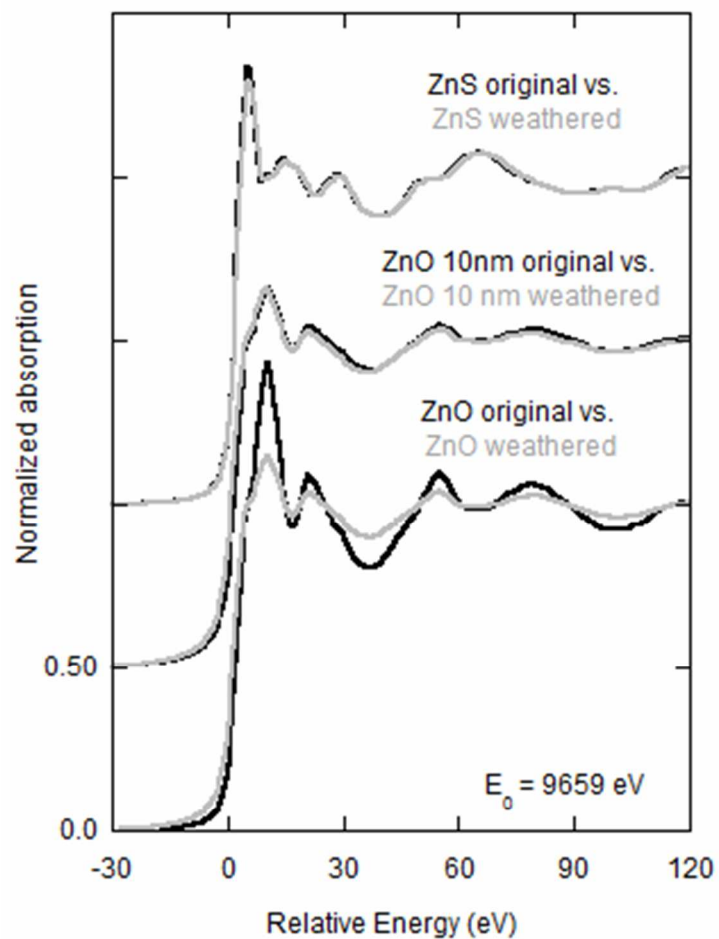
Figure A11. Zn K-XANES spectra (top left) and XRD patterns (right) comparing the original (black line) to the weathered (grey line) reference compounds of ZnO (mesh powder), ZnO 10 nm particles and ZnS (mesh powder). Arrows in the XRD pattern for weathered ZnO 10 nm indicate Zn hydroxide carbonate.

S18
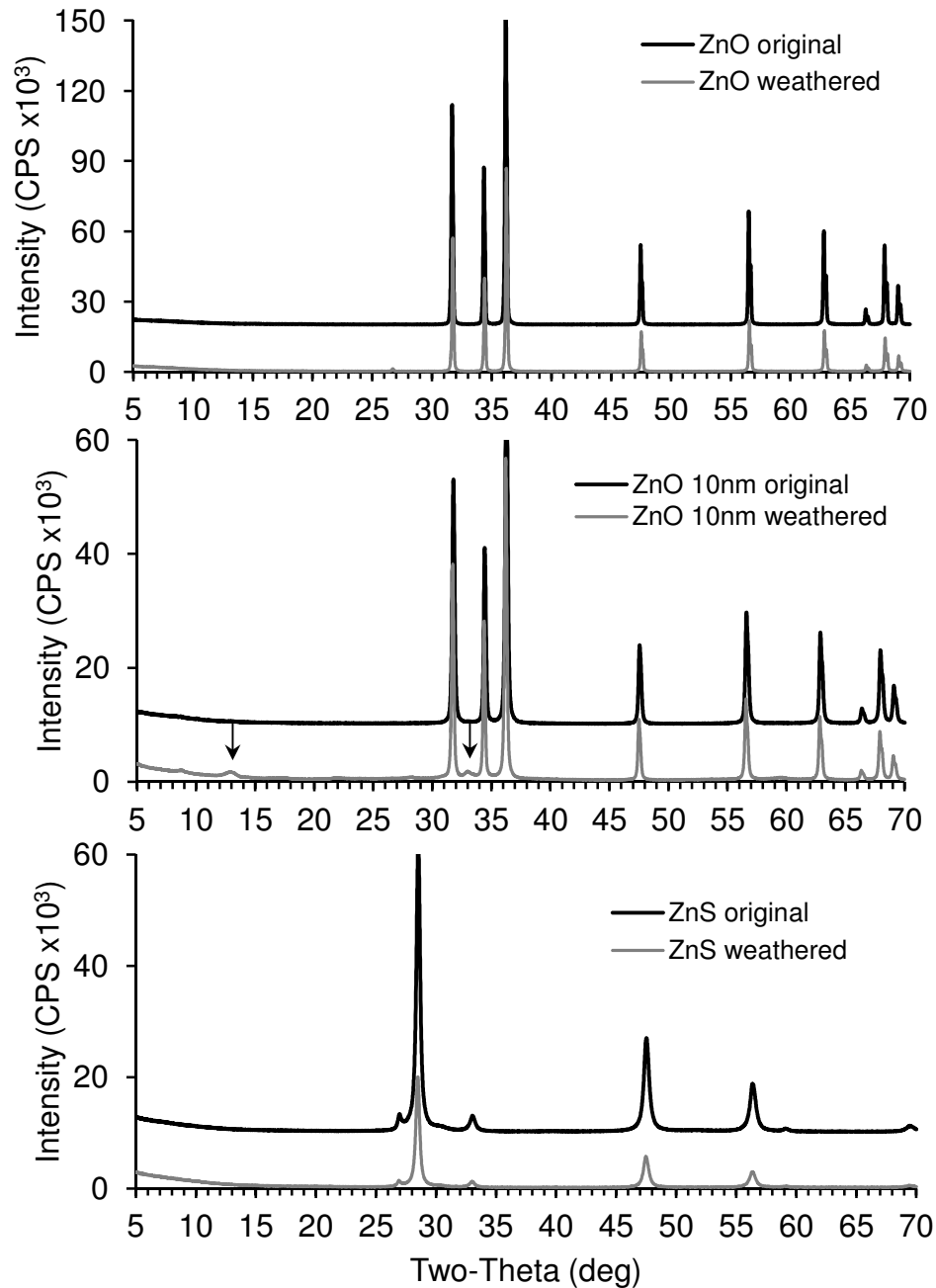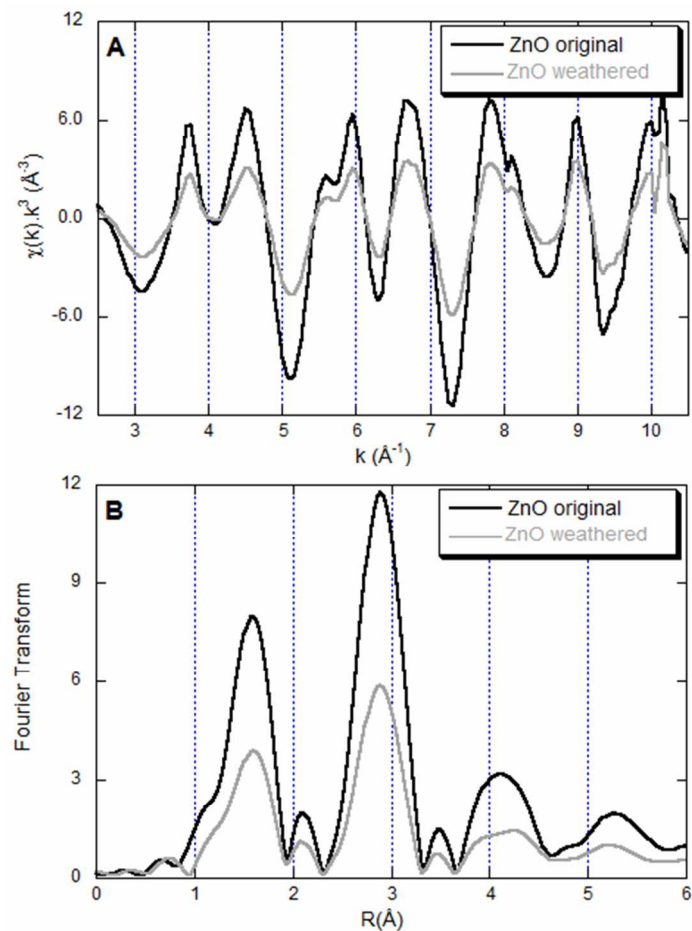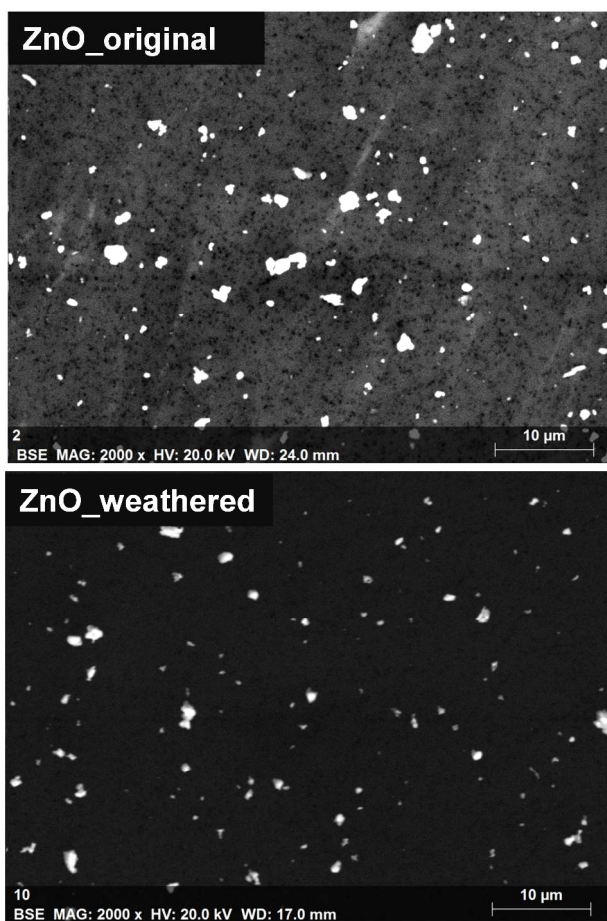
Figure A12. BSE images of ZnO mesh powder after suspension in propanol, dispersion in ultrasonic bath and filtration on Nucleopore 0.1 µm (left) and EXAFS chi and FT spectra (right) comparing the ZnO mesh powder before (black line) and after 5 months of weathering (grey line). BSE images would suggest a slight decrease in grain size for ZnO after 5 months of weathering. A significant decrease in the amplitude of EXAFS oscillations is observed after 5 months of weathering. These results remain to be investigated more in-depth but suggest structural change possibly due to chemisorbed water molecules at the ZnO surfaces and/or decrease in particle size during weathering. Similar reduced amplitude in the EXAFS oscillations was observed for the original ZnO 10 nm particle (Figure A1). For ZnO powder particles, the ZnO($10\bar{1}0$)-surfaces are dominant and were shown to chemisorb water molecules at the coordinately unsaturated Zn site, each unit cell being able to accommodate one intact and one dissociated water molecule (Wöll, 2007). Chemisorbed water would not be removed by air-drying as high temperature is required to remove these molecules.

REFERENCES

Beauchemin, S., L. MacLean and P. Rasmussen. 2011. Lead speciation in indoor dust: A case study to assess old paint contribution in a canadian urban house. Environ. Geochem. and Health 33:343–352.

Beauchemin, S., D. Hesterberg, J. Nadeau, and J. C. McGeer. 2004. Speciation of hepatic Zn in trout exposed to elevated waterborne Zn using X-ray absorption spectroscopy. Environ. Sci. Technol. 38: 1288 – 1295.

Beauchemin, S., D. Hesterberg, J. Chou, M. Beauchemin, R. R. Simard, and D. Sayers. 2003. Speciation of phosphorus in P-enriched agricultural soils using XANES spectroscopy and chemical fractionation. J. Environ. Qual. 32:1809-1819.

Beauchemin, S., D. Hesterberg and M. Beauchemin. 2002. Principal component analysis approach for modeling sulfur K-XANES spectra of humic acids. Soil Sci. Soc. Am. J. 66: 83-91.

Beak, D.G., N.T. Basta, K.G. Scheckel and S.J. Traina. 2008. Linking solid phase speciation of Pb sequestered to birnessite to oral Pb bioaccessibility: Implications for soil remediation. Environment Science and Technology. 42: 779-785.

Ford, R. G. and D. L. Sparks, 2000. The nature of Zn precipitates formed in the presence of pyrophyllite. Environ. Sci. Technol. 34: 2479-2483.

Hayes, S.M., P.A. O'Day, S.M. Webb, R.M. Maier and J. Chorover. 2011. Changes in zinc speciation with mine tailings acidification in a semiarid weathering environment. Environ. Sci. Technol. 45: 7166-7172.

Manceau, A., M.A. Marcus and N. Tamura. 2002. Quantitative speciation of heavy metals in soils and sediments by synchrotron X-ray techniques. In *Applications of Synchrotron Radiation in Low-Temperature Geochemistry and Environmental Science*; Fenter, P., Sturchio, N.C., Eds; Mineralogical Society of America: Washington, DC 2002; pp 579.

Ravel B., M. Newville. 2005. ATHENA, ARTEMIS, HEPHAESTUS: Data analysis for X-ray absorption spectroscopy using IFEFFIT. J. Synchrotron Rad. 12: 537-541.

Schwertmann, U. and R. M. Cornell. 1991. *Iron Oxides in the Laboratory*. VCH Publishers, Weinheim, Germany. (pp. 90-94).

Taylor, R.M. 1984. The rapid formation of crystalline double hydroxy salts and other compounds by controlled hydrolysis. Clay Miner. 19: 591 – 603.

Wöll, C. The chemistry and physics of zinc oxide surfaces. 2007. Prog. Surf. Sci. 82: 55-120.